Integration of Altimetry and Interferometry Techniques for the Identification of the Potential of New Marsh Areas in Iraq

Murtadha Aryan
Geospatial Imaging and Information Research Group, Faculty of Built Environment and Surveying, Universiti Teknologi Malaysia, Skudai, Malaysia
aryan@graduate.utm.my (corresponding author)

Abd Wahid Bin Rasib
Geospatial Imaging and Information Research Group, Faculty of Built Environment and Surveying, Universiti Teknologi Malaysia, Skudai, Malaysia
abdwahid@utm.my

Muhammad Imzan Bin Hassan
Geospatial Imaging and Information Research Group, Faculty of Built Environment and Surveying, Universiti Teknologi Malaysia, Skudai, Malaysia
imzan@utm.my

Mohammad Hanif Bin Hamden
Geospatial Imaging and Information Research Group, Faculty of Built Environment and Surveying, Universiti Teknologi Malaysia, Skudai, Malaysia
mohammad.hanif@utm.my

Received: 21 October 2025 | Revised: 12 November 2025, 1 December 2025, 18 December 2025, 24 December 2025, and 30 December 2025 | Accepted: 3 January 2026

 DOI: https://doi.org/10.48084/etasr.15691

ABSTRACT

Identifying potential marsh areas in Iraq is essential for sustainable water resource monitoring in arid regions. This study uses altimetry, interferometric synthetic aperture radar techniques, and hydrological modeling for identifying potential marsh sites in the southwestern Iraq desert. In the study's methodology, altimetry data were used to provide precise Euphrates water elevations, while Interferometric Synthetic Aperture Radar (InSAR)-derived elevation enhanced the spatial detail of the Digital Elevation Model (DEM). A stream burning technique was applied to improve DEM-2024 and ensure accurate hydrological representation. This integration enabled the generation of a high-resolution topographic model capable of identifying low-lying zones with high potential for marsh restoration. Three DEMs from 2022, 2023, and 2024 were evaluated for accuracy using Real-Time Kinematic (RTK) points. DEM 2024, enhanced by the stream burning technique, was the most accurate, with a Root Mean Square Error (RMSE) of 3.27 m, a bias of -0.86 m, and a Standard Deviation (SD) of 3.15 m. This improved DEM facilitated the reliable identification of potential marsh boundaries. The Euphrates River discharge value at 31.3351°N, 45.0527°E was 549.95 m^3/s, which was the basis for hydrological simulations. Moreover, the channel characteristics (64.7 m width, 5.0 m depth, and 1.7 m/s velocity) validated the viability of water diversion for marsh creation. Geomorphological assessments identified basin 280 as the most suitable site for creating a marsh. With a total area of 725.74 km^2, river length of 301,647.5 m, elongation ratio of 0.589, and circularity ratio of 0.650, it indicates favorable hydrological retention and flow distribution characteristics. This study demonstrates the integration of remotely sensed altimetry techniques, DEM optimization, and hydrological analysis to support large-scale marsh identification and restoration.

Keywords-altimetry; interferometry; integration; marsh; stream-burning; Iraq

I. INTRODUCTION

Accurate topographical data are crucial for hydrological and geomorphological studies, especially in the southwestern desert regions of Iraq, because subtle elevation changes directly control how water is distributed and how wetlands are formed and located [1]. Authors in [2, 3] noted that although DEM serves as the basis for many hydrological investigations, radar signal distortions, vegetation, and water surface reflections often compromise its accuracy in flat terrain. Owing to the flexibility of SAR, the InSAR technique is scientific and practical for deriving DEMs [4]. Furthermore, although InSAR has the advantages of a large region and continuous space coverage, the InSAR-DEM generation process is extremely susceptible to various factors, such as the selection of the interference pair, baseline, and atmospheric environments [5]. Moreover, authors in [6] showed that DEM generated using the InSAR technique performs best in arid and semi-arid areas. It is Authors in [7] demonstrated that the use of high-quality Ground Control Points (GCPs) in the orbit refinement and reflattening process can correct the baseline parameters and remove the flattening effect to improve the DEM accuracy.

Increasing DEM accuracy is necessary to improve floodplain dynamics, flow direction, and water body delineation. An efficient technique for enhancing hydrological modeling is the stream burning strategy, which draws and determines drainage networks on DEMs. The hydrological consistency and connection of the modeled topography were ensured by utilizing the stream burning technique, which hydrologically enforces drainage channels inside the DEM [8]. In the same context, by inventing the Topological Breach Burn technique, authors in [9] applied the stream burning strategy to improve the hydrological accuracy of drainage networks produced from DEM. It guarantees hydrologically consistent flow routes and minimizes problems like stream piracy. This technique produces more realistic river network delineations and flow routing by maintaining precise drainage divides and watershed borders, even at coarse resolutions, greatly enhancing the scale sensitivity and reliability of DEM-based hydrological modeling.

However, recent advancements in satellite altimetry have revolutionized surface water and terrain mapping by providing water elevations for inland water. New perspectives for measuring water surface elevation at ungauged sites were opened with the launch of Sentinel-3A on 16th February 2016. With an along-track resolution of approximately 250 m, Sentinel-3A possesses great potential for monitoring the water levels of inland water bodies [10]. The Ogooué River and the Inner Niger Delta were studied using water levels obtained from a few altimeters, including Sentinel-3A [11, 12]. It was found that Sentinel-3A had less than 0.41 m RMSE when using in situ data as a benchmark [11]. However, the Open-Loop Tracking Command (OLTC) demonstrated positive performance and perfect quality for upcoming measurement possibilities for Sentinel-3A to obtain the water level time series for narrow-width rivers [13].

One of the largest and most biologically significant wetland ecosystems in the world is the marshlands in southern Iraq, also known as the "Heart of the Mesopotamian Civilization" [14]. Hydrological and biological changes have led to an increase in desert areas in southern Iraq, which affects the processing of the elevations in these areas. Therefore, for surface hydrology, drainage connections, and inundation dynamics to be effectively represented, a sophisticated DEM is necessary. To increase the vertical accuracy and hydrological realism of DEMs, this study proposes integrating satellite altimetry and InSAR data. Moreover, the integration of these technologies (altimetry and interferometry) allows for an improved understanding of hydrological processes in data-scarce regions, such as Iraq, where these locations suffer from desertification due to political instability and environmental challenges [15]. While interferometry delivers high spatial resolution and sensitivity to minute topographic differences, altimetry provides accurate elevation data over water surfaces [16]. This combination improves the depiction of water flow networks, especially in marsh and floodplain systems, and fixes DEM errors brought on by radar noise or vegetation interference. The ultimate goal of this method is to create a high-resolution, hydrologically conditioned DEM that will enhance marshland identification, mapping, and monitoring in Iraq, supporting adaptive water management and wetland restoration initiatives in the face of changing climate conditions.

Building on the analysis of Manning's coefficient variations in the Al-Adhaim River Basin [17], this study extends this approach to calculate the discharge in the Euphrates River. By integrating the derived hydraulic roughness values with cross-sectional geometry, slope, and flow depth data in Manning's equation, discharge can be accurately quantified under varying climatic and land-use conditions. Additionally, this process improves the understanding of hydraulic dynamics in arid regions and supports effective water resource management and desertification control strategies along the banks of the Euphrates River. The results of the current study show that at the location (31.3351°N, 45.0527°E) for the new channel on the Euphrates River identified by the altimetry technique, the water velocity was 1.7 m/s, and the discharge value was 549.95 m^3/s, with a cross-sectional size of 323.5 m^2. The new channel will supply water to a desert area to create a new potential marsh area in southwestern Iraq. Several basins were also determined, but the most significant one was that with ID 280, which hydrological and geomorphological studies indicated as the best place for the marsh to expand.

Although some studies have focused on integrating techniques, there has been no research on the integration of discharge-based hydrological modeling based on the altimetry technique and InSAR data, which used a stream burning approach to enhance DEM accuracy for identifying potential marsh areas in the southwest of Iraq, leaving a gap in understanding the region's topographic and hydrological dynamics. Consequently, the objective of this study is to identify potential marsh areas in the southwestern desert of Iraq by integrating altimetry and interferometric data using a stream burning approach to enhance DEM precision for the study area.

In general, this study investigated the precision and suitability of data analysis that integrates two key techniques (interferometry and altimetry) by applying the stream-burning approach to identify a potential new marsh region for reducing the effects of desertification in southwestern Iraq. Furthermore, the primary contributions of this study are: (i) the focused collection of real-ground data as well as the capture of data at the Euphrates River and the desert in southwest Iraq, (ii) the demonstration of the benefit of using stream-burning to improve the precision of the DEM produced by the InSAR technique, (iii) utilization of the rigorous geographic cross-validation offered by VSs, gauging stations, and GCPs RTK points (iv) to identify potential marsh regions in Iraq. The latter is also consistent with efforts to address the issue of desertification, which has become a major problem in Iraq [18] and is regarded as the most difficult environmental issue that directly threatens food security [19]. The findings can also serve as a local starting point for tracking water resources in arid and semi-arid regions. Furthermore, it represents a considerable challenge for water resource management, especially with demand increasing in other sectors. At both local and regional scales, it offers new analytical skills for water resource management planners to improve decision making [20].

II. MATERIALS AND METHODS

A. Study Area

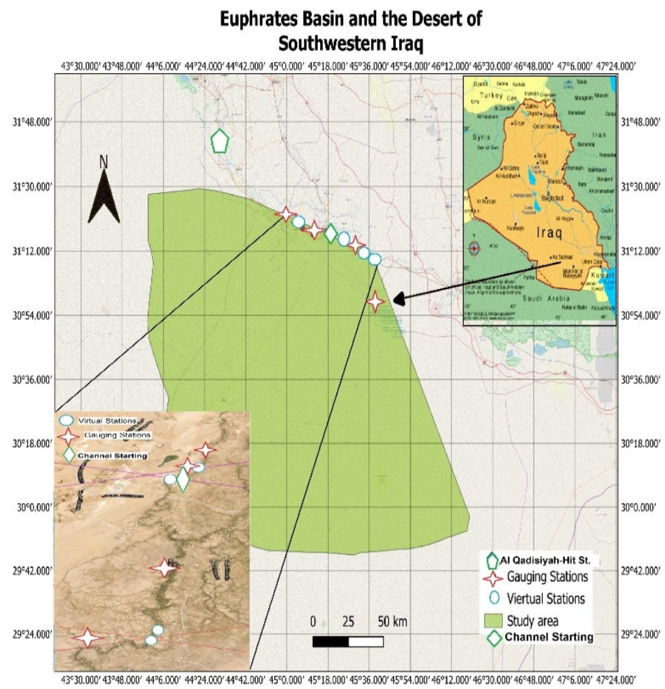

Fig. 1. The Iraqi southwest desert and the Euphrates basin.

The research area comprised two contiguous sections in southern and southwestern Iraq. The first is the southern portion of the Euphrates River, and the second is the region that stretches into the southwest of the Iraqi desert, where marshes can be identified. This arid region is characterized by extreme summer temperatures exceeding 50 °C and an annual precipitation of less than 150 mm. The 11,971.85 km^2 area has geomorphological characteristics, such as naturally occurring depressions and gently sloping alluvial plains, which aid in water retention despite its challenging terrain.

The dual-region study area technique ensures a comprehensive hydrological evaluation by integrating remote sensing data with in situ observations from gauging and GCPs (Figure 1). The proximity of gauging stations to Virtual Station (VS) locations improved the discharge validation for the Euphrates River. At the same time, topography appropriateness in the south-western desert (Top Left 31.440911° N45.150375 ° E, Bottom Left 31.304669° N44.297403 ° E, Top Right 30.624492° N44.135336 ° E, Bottom Right 30.762158° N45.298614 ° E) (Figure 1) encourages sustainable marsh reestablishment.

B. Data Acquisition (Satellite and In-Situ Dataset)

1) In-Situ Data

a) Altimetry Data (Gauging Stations)

This study used an altimetry dataset for four VSs obtained from the Database for Hydrological Time Series of Inland Waters (DAHITI) website. A list of all VSs, adjacent gauging stations, and their distances in the research region is provided in Table I. Moreover, this investigation utilizes the altimetry technique, guided by gauging stations (Al-Hamza, Al-Rumaitha, Al-Khether, and Al-Rumaila stations) located along the Euphrates River.

TABLE I. THE VSS FOR SENTINEL-3, USED IN THIS STUDY, ALONG WITH THEIR NEARBY GAUGING STATIONS

VS ID from DAHITI	Gauging station			
	Al-Hamza	Al-Rumaitha	Al-Khether	Al-Rumaila
41508	3.060 km			
41509		29.870 km		
24448			14.990 km	
41512				35.890 km

b) Ground Control Points (RTK)

Ground survey points (RTKs) in the study area were selected based on their accessibility, stability, and ability to provide a spatial distribution of different terrain features (Figure 2). The survey points span across the study area in southern Iraq with specific elevations and accurate geolocation.

High-precision coordinates and elevations for the survey locations within the research region were obtained using a single-based RTK GNSS system. Centimeter-level positional precision was made possible by the system's stationary base station and rover unit. Through a UHF radio connection, differential adjustments were transmitted in real-time from the base station to the rover, enabling prompt positional data correction during field observations. While the rover gathered positional data at each assigned survey site, the base station was set up over a known reference point to guarantee the accuracy of the sent adjustments. Ground-based reference sites were created inside the research region and surveyed/examined using static GNSS techniques to verify the accuracy of the RTK observations. These reference points served as control points for the quality assurance and accuracy evaluation of the collected data.

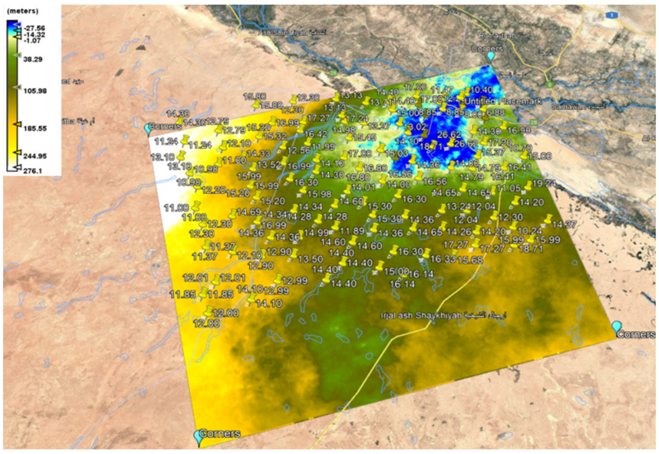

Fig. 2. The RTK points projected on the DEM for the study area.

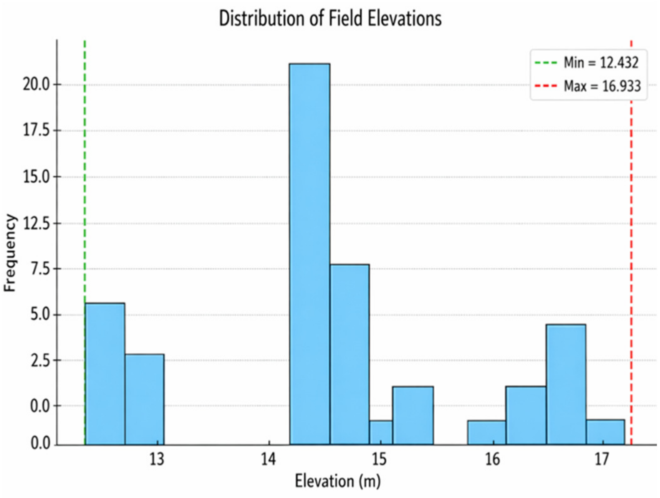

Fig. 3. The elevation range of the RTK points' field heights for the study area.

Figure 3 displays the range and distribution of field elevation measurements collected in the study area. The latter contained 60 RTK points. With a minimum elevation of 12.3 m and a maximum elevation of 16.933 m, the elevation range was 4.633 m. This range indicates significant topographic variability across the landscape, enabling the evaluation of potential marsh areas and modeling of surface hydrology. The majority of the elevation data were found in the range's core, which showed largely flat terrain with minor variations. Accurately capturing this elevation variation is essential for producing reliable DEMs and supporting sustainable land development planning.

2) Satellite Data

a) Sentinel-3 Data

In this study, the water level of the Euphrates River in Iraq was measured using satellite altimetry and time-series datasets from DAHITI. The Sentinel-3A and B pass numbers over the Euphrates Basin (0225b, 0326a, 0225a, and 0326a) (Table II) had the best coverage over the Euphrates River study area.

TABLE II. INFORMATION ON THE DAHITI POINTS USED IN THIS STUDY

DAHITI-ID	Coordinates	# Data points	Time coverage	Water level range (m)
41508	31.3520°N, 45.0311°E	53	2018 – 2024	~8.5 – 11.0
41509	31.3147°N, 45.0586°E	49	2018 – 2024	~8.5 – 11.1
24448	31.2885°N, 45.5161°E	68	2018 – 2024	~4.2 – 6.8
41512	31.2878°N, 45.5188°E	60	May 17, 2016 – Feb 20, 2024	4.205 – 6.941

b) Sentinel-1 Data

Sentinel-1A&B from the Alaska Satellite Facility (ASF) provided the Level-1 ground range detected images utilized in this investigation, which are part of the IW mode with VV polarization, across the study region between January 2022 and September 2024 (Table III). Furthermore, there was no need to create a mosaic, as the entire region of the Euphrates River could be seen in a single shot. Table IV lists the Sentinel-1 images used in this study.

TABLE III. THE CHARACTERISTICS OF SENTINEL-1 IMAGES USED IN THIS STUDY

Study period	01/01/2022-23/09/2024
Level	1
Format	SLC
Swath width	250 km²
Mode	IW
Polarization	VV+VH
Spatial resolution	5 m x 20 m
Data Source	ASF
Temporal range	Revisit time is ~6 days (combined constellation); Sentinel-1B is now inactive for ~12 days.
Incidence angle range	29.1° - 46.0°

TABLE IV. THE IMAGES FOR THE IMPLEMENTATION OF THE INTERFEROMETRY TECHNIQUE

Satellite	Acquisition date	Data type/ mode	Pass direction	Remarks
Sentinel-1A	01/01/2022	SLC-IW	Descending	Quick- Look
Sentinel-1A	13/01/2022	SLC-IW	Descending	Quick-Look
Sentinel-1A	29/9/2023	SLC-IW	Descending	Quick-Look
Sentinel-1A	11/10/2023	SLC-IW	Descending	Quick-Look
Sentinel-1A	11/09/2024	SLC-IW	Descending	Quick-Look
Sentinel-1A	23/09/2024	SLC-IW	Descending	Quick-Look

III. VALIDATION OF WATER LEVEL TIME SERIES FOR VIRTUAL STATIONS BY GAUGING STATIONS

DAHITI stations include VS 41509, 24448, and 41512 (corresponding to the Al-Rumaitha, Al-Khithir, and Al-Rumaila stations, respectively), and station ID 41508 (31.352 ºN, 45.0311 ºE), which is located 3.06 km upstream of the Al-

Hamza gauging station (Table I). With river widths ranging from 45 to 105 m, these stations generated almost 200 altimetry observations. All data were examined, along with a detailed analysis of seasonality, between-annual variations, and water levels, all of which are necessary to determine the ideal intake location for the proposed canal system.

A. Statistical Evaluation and Accuracy Assessment of Water Level Data at the Gauging Station and Virtual Stations

In this study, a thorough statistical analysis was performed using (1-6) to compare the WSE of the gauging stations (al-Hamza, al-Rumaitha, al-Khether, and al-Rumaila) with their closest DAHITI VSs. This process was used to analyze the DEMs. Descriptive statistics (mean, standard deviation, and range), correlation analysis (Pearson correlation to ascertain the relationship between the two datasets), error metrics (RMSE and mean absolute error), and graphical representation (verbose time series plot and scatter plot with a trend line) were used for the analysis:

$$RMSE = \left(\sum_{\text{i}}^{N} \frac{(H(gauge)\text{i} - H(altimety)\text{i})^2}{N}\right)^{1/2} \quad (1)$$

$$MAE = \frac{1}{n}\sum_{i=1}^{n} |\ Zi^{obs} - Zi^{model} \quad (2)$$

$$r = \frac{\sum_{i-1}^{n}(\chi i - X^{-})(Y - \bar{Y})}{\sqrt{\sum_{i-1}^{n}(\chi i - X^{-})^2}\sqrt{\sum_{i-1}^{n}(Y - \bar{Y})^2}} \quad (3)$$

$$Mean = \frac{1}{n}\sum_{i=1}^{n}[Zi^{obs} - Zi^{model}] \quad (4)$$

$$\sigma = \sqrt{\frac{1}{n}\sum_{i-1}^{n}(Xi - \chi)^2} \quad (5)$$

The range in = maximum value - minimum value(6)

B. Estimation of River Discharge from Satellite Radar Altimetry (Quantitative Analysis of Discharge)

In central Iraq, at a place called Al-Qadisiyah-Hit, which is 39 km north of the Al-Hamza gauging station, the average annual outflow is approximately 356 m^3/s. Given that the width of the river in this part extends from the center to southern Iraq and ranges between 50 and 300 m:

Velocity (m/s) = discharge (m^3/s) / (width × depth) (7)

Assuming an average depth of 5 m, then the estimated velocity is:

Velocity ≈ 356 m^3/s / (250 m × 5 m) ≈ 0.285 m/s

1) Hydrological Estimation and Feasibility Assessment for Canal Creation at Coordinate Point (31.3351°N, 45.0527°E) on the Euphrates River

Since the average width is 64.7 m and the average depth is 5 m, (7) can be applied and the velocity of water flowing in the Euphrates River at the location of 31.3351 ºN latitude and 45.0527 ºE longitude between the gauging stations of AL-Hamza and Al-Rumaitha can be estimated.

The construction of the upstream dam at this location was the main cause of the mean daily discharge shifting from 967 m^3/s to 553 m^3/s after 1985. Using all relevant information (width, depth, and velocity), the discharge at the research site was estimated.

2) Hydrological Estimation and Feasibility Assessment for the Second Potential Section (31.314, 45.351) between Al-Rumaitha and Al-Khether Gauging Stations

The discharge (Q) at point no. 4 (the second point at (31.314, 45.351)) was determined using the Manning equation and open-channel flow, as expressed in:

$$V = \frac{1}{n}R^{\frac{2}{3}}S^{\frac{1}{2}} \quad (8)$$

$$Q = \frac{1}{n}AR^{\frac{2}{3}}S^{\frac{1}{2}} \quad (9)$$

Finally, the combination of hydrological modeling and Geographic Information System (GIS)-based spatial analysis supports the proposed water route, making it topographically and hydrologically feasible. It helps identify the best locations and reduces erosion, water loss, and unsustainable divergence.

IV. GENERATION AND OPTIMIZATION OF DEM FOR THE STUDY AREA

Using the stream-burning methodology, altimetry and interferometry were combined to provide a precise and dependable method for monitoring and supporting the restoration of the Mesopotamian marshlands in southwestern Iraq. In order to mitigate the impacts of desertification and restore this ecosystem, the InSAR methodology was adopted, which can offer prompt and comprehensive information on the changes to the land surface.

A. Enhancement of DEM 2024's Hydrology by the Stream Burning Approach

Applying the stream burning technology, altimetry-adjusted water levels were bolstered with InSAR-created DEM level information to improve hydrological flow courses more accurately. Such a method maintains hydrological realism in the modeling of the water flow and corrects the DEM by inserting river channels into a terrain model. Moreover, the stream burning helps align the forecasted flow paths with actual river networks and eliminates the inherent limitations of DEM.

B. Phase Quality Assessment and Filtering

In this step, after applying several techniques to the data, including phase unwrapping, noise removal, and elimination of atmospheric and orbital errors, a continuous signal of deformation was generated that reflected the real-world surface displacement as a function of time. This eliminated the wrapped part (it oscillated between negative and positive p), representing a better view of the actual displacement. Furthermore, the phase was denoised by employing methods, such as Goldstein filtering and Minimum Cost Flow (MCF) unwrapping, which improved the strength of the interferometric phase. This enhanced the overall accuracy of the derived surface displacement. Moreover, corrections for atmospheric disturbances (regarding external atmospheric models such as SRTM records) and orbital errors (concerning precise satellite orbit data) were applied, thereby minimizing the impact of the InSAR measurement by eliminating these errors.

C. Enhancement and Verification of Interferometric Phase Measurements: The RTK Surveys

To obtain the statistical accuracy of elevations for the DEM and altimetry data in the study area, this investigation compared data obtained from satellites with GCPs (RTKs) using the key statistical indicators: RMSE, which measures the overall accuracy of elevation bias, mean error, which is an indication of systematic overestimation or underestimation, and SD, which represents the distribution of elevation differences.

V. UTILIZING HYDROLOGICAL MODELING AND GIS TO FIND POTENTIAL MARSH AREAS

GIS-based spatial and hydrological modeling is important for evaluating the possibility of forming marshlands in the southwestern desert of Iraq. This involves simulating water flow, identifying suitable locations for water storage, and analyzing potential hydrological connections using a DEM and remote sensing information.

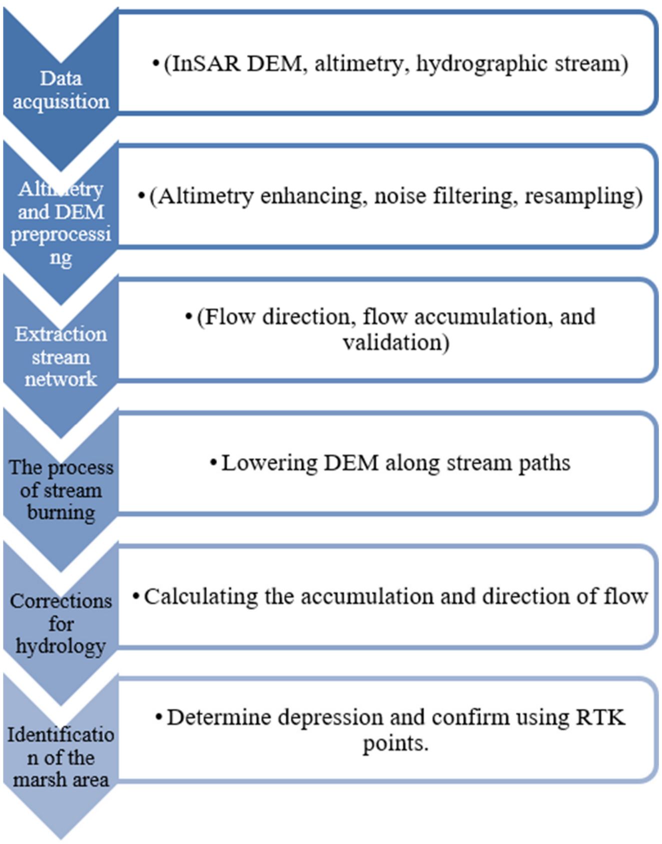

Fig. 4. Flowchart of the study.

This study revealed the flow paths and zones of accumulation. Nonetheless, before carrying out these procedures, the DEM pre-processing procedure to correct the depressions and abnormalities, i.e., the sink filling, must be carried out to present a realistic modeling of water flow. The flowchart of the methodology for determining the marsh area using Sentinel satellite missions is shown in Figure 4.

VI. RESULTS

A. Quantitative Evaluation of Virtual and Gauging Station Data for Hydrological Assessment (Water Level Variations from Altimetry Data)

When changes in water levels play a significant role in the stability of an ecosystem, such as the Euphrates River, it is possible to monitor water level fluctuations and identify potential new marshes in Iraq using DAHITI VSs. When they are used with gauging stations of the Euphrates River, they improve the evaluation of the hydrological models and facilitate successful decision-making regarding the restoration and management of wetlands.

1) Statistical Evaluation and Accuracy Assessment of Water Level Data at the Gauging Station and Virtual Stations

The elevation changes of 32 observations over four monitoring sites (Al-Hamza, Al-Rumaitha, Al-Khether, and Al-Rumaila) are depicted in Figure 5. Elevation variability is displayed comparatively on a line graph, which also allows for the observation of geographical and temporal variations between places. Throughout the measurement, Al-Hamza exhibited little fluctuation and maintained a comparatively constant level of 10.5 m. This homogeneity points to minimum measuring error, negligible vertical displacement, and a geologically stable region. Technically, Al-Khether and Al-Rumaitha differ to some extent. Al-Rumaitha's elevation runs from 7.5 to 10 m, whereas Al-Khether's ranges from 4.5 to 9.5 m. These patterns may indicate regional subsidence, seasonal volatility, or differences in data collection over external variables. Al-Rumaila's modest elevation fluctuations, which vary from 6.5 to 8.5 m, are indicative of either a possible hydrological mechanism or mid-level topographic variability.

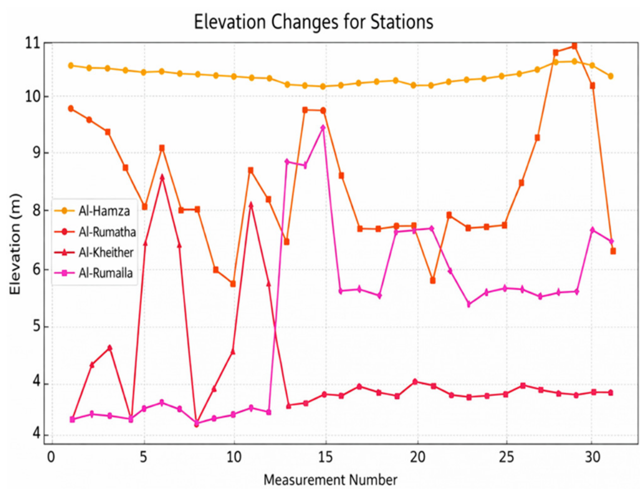

Fig. 5. The elevation changes of gauging stations.

There are differences in accuracy and correlation between the four gauging stations on the Euphrates River (Al-Hamza, Al-Rumaitha, Al-Khuther, and Al-Rumaila) and the DAHITI

VSs. Although there was a statistically significant linear association between the DAHITI VS and Al-Hamza gauging station (Pearson r = 0.75, R^2 = 0.54), the DAHITI station was consistently under-measured by around 1.53 m compared to the data from Al-Hamza gauging stations (Figure 6). This trend is biased when combined with the corrective variables. Table V shows the results based on all the gauging stations and VSs used in this investigation. Furthermore, Figures 6-9 illustrate the relationships between these variables.

TABLE V. STATISTICAL ANALYSIS RESULTS, CORRELATION ANALYSIS, AND ERROR ANALYSIS FOR GAUGING STATIONS AND VSS

Metric	**Virtual versus Al-Rumaila**	**Virtual versus Al-Khether**	**Virtual versus Al-Rumaithe**	**Virtual versus Al-Hamza**
Mean (virtual)	5.30 m	4.554 m	8.86 m	8.83 m
SD (virtual)	0.74 m	0.293 m	0.17 m	0.34 m
Pearson correlation coefficient	0.57 (moderate positive)	-0.189 (inverse relationship)	0.41 (moderate correlation)	0.75 (moderate to strong)
p-value	0.0009 (significant)	0.326 (not significant)	0.048 (moderate correlation)	0.00001 (significant correlation)
RMSE	1.59 m	1.450 m	1.03 m	1.58 m
MAE	1.09 m	0.952 m	0.86 m	1.55 m

In the same context, the DAHITI VS (ID 41509) seems to provide more consistent data with a smaller range, with a slightly higher mean of 8.86 m and a substantially lower SD of 0.17 m (Table V). The two datasets were positively correlated because the Pearson correlation coefficient of 0.41 indicates that increases in the DAHITI dataset are usually accompanied by elevations in the water level of the Al-Rumaitha station (Figure 7). This is based on a p-value of 0.048, which is less than 0.05 and shows that a connection has been established, even if it is not significantly linear.

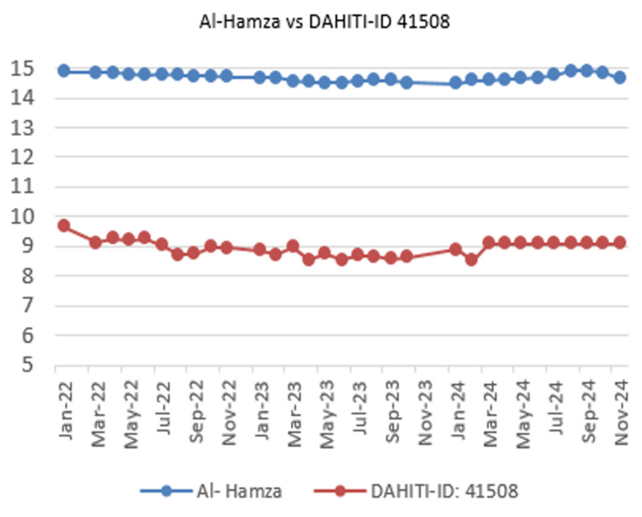

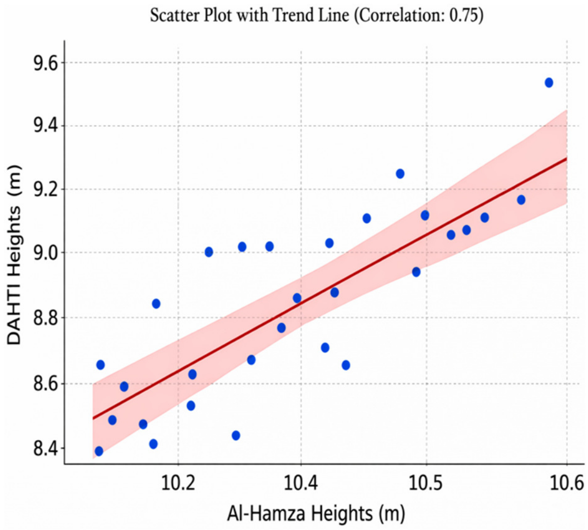

Fig. 6. Comparison of height and the relationship between water levels at the AL-Hamza gauging station and the VS.

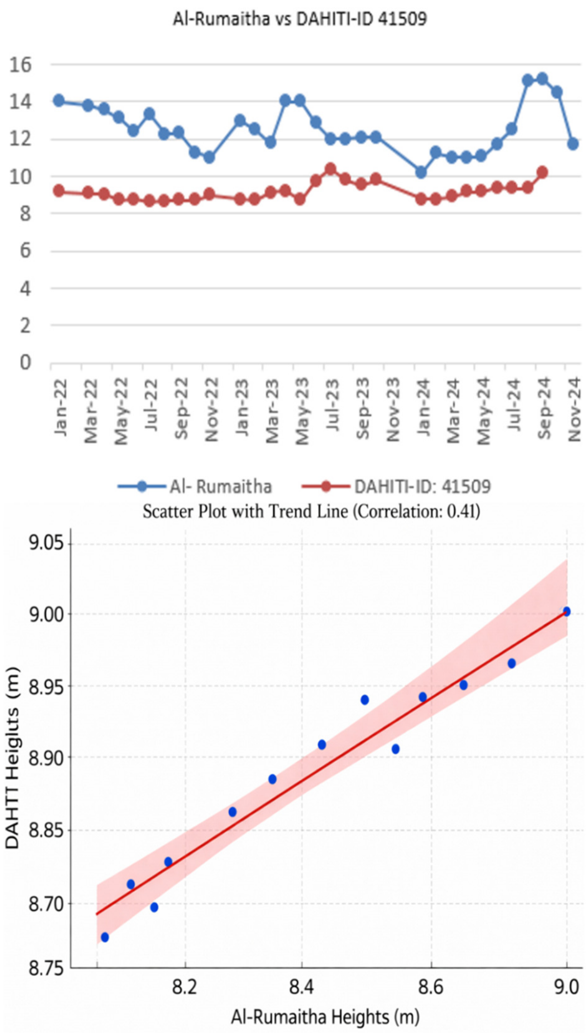

Fig. 7. Comparison of height and the relationship between water levels at the AL-Rumaitha gauging station and the VS.

Conversely, the Pearson correlation coefficient of 0.189 (Table V) shows a weak inverse link despite the clear negative correlation, while the relationship's non-significance is supported by its p-value of 0.326. It implies that rather than having a genuine underlying connection, two variables could merely have an indirect link. The coefficient of determination (R^2)), which was computed to be around -0.563 (Figure 8), further demonstrated the insufficient ability of the DAHITI data to explain the variability of the Al-Khuther observations. Since the model did not fit the observed data as well as the average of the observations, the R^2 value was negative, which is unusual.

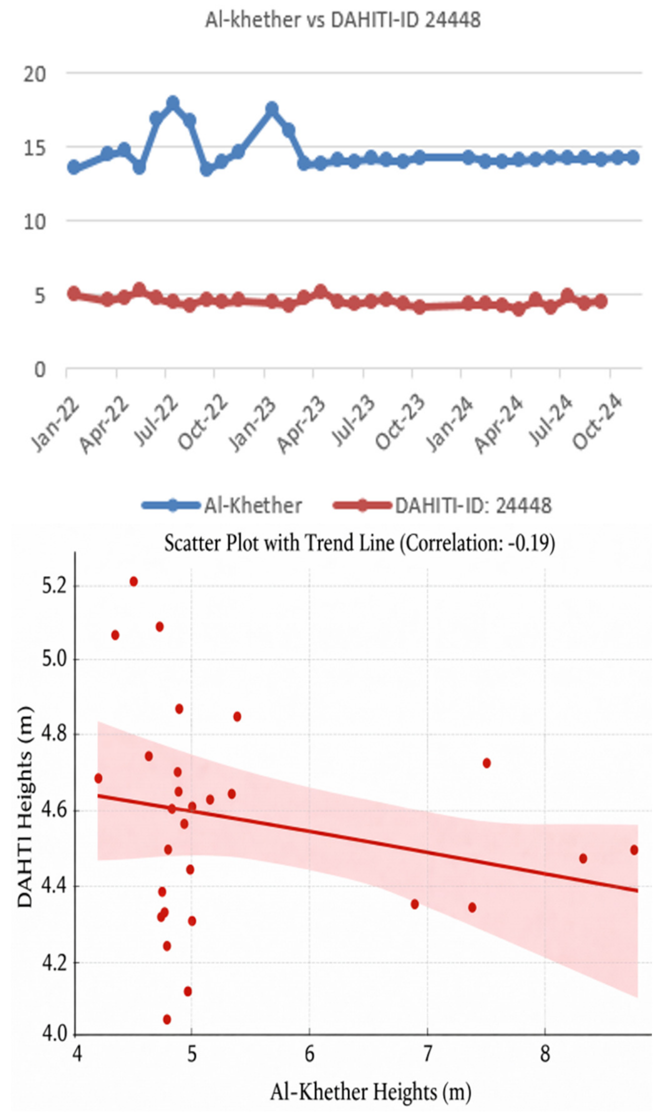

Fig. 8. Comparison of height and the relationship between water levels at the AL-Khether gauging station and the VS.

However, a positive correlation was observed between the Al-Rumaila gauging station and the DAHITI VS (ID: 41512), with a Pearson's correlation coefficient of 0.57. The association is quite high and unlikely to be the result of chance because the first number is 0.0009 (Figure 9). The R^2 value of 0.32 indicates that the 32 % fluctuation in the DAHITI data can only be attributed to in situ measurements, suggesting that there must be other characteristics that satellite altimetry cannot measure (Table V). A comparatively favorable correlation of 0.57 is shown by the red trend line with a dashed range of confidence. This implies that the heights of DAHITI and Al-Rumaitha are likely to rise simultaneously.

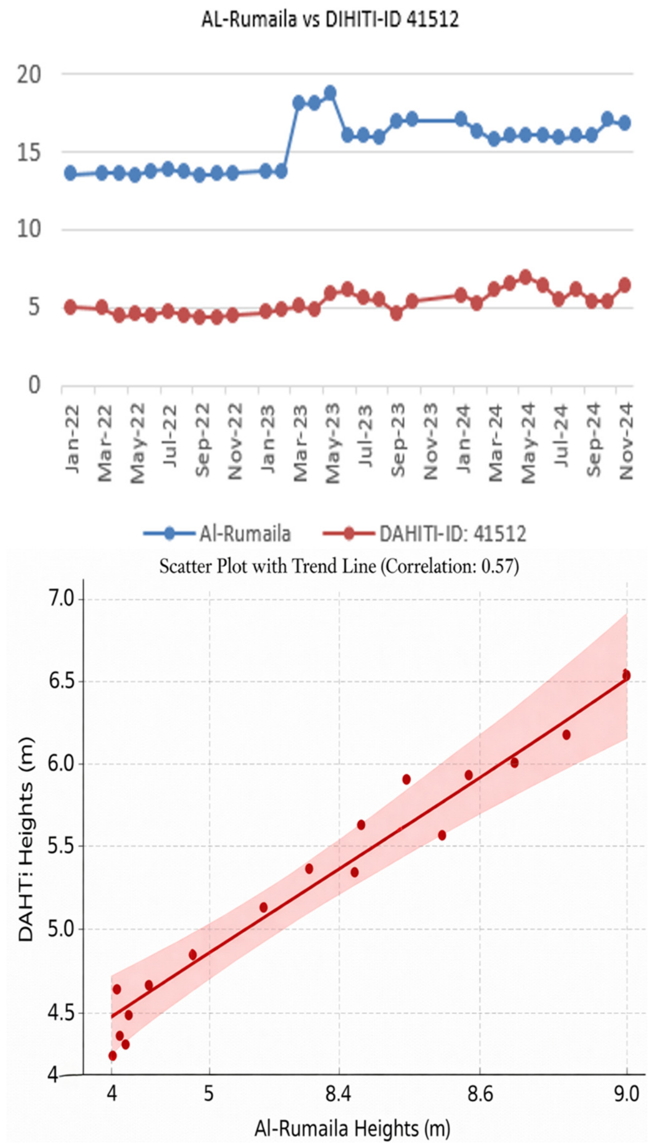

Fig. 9. Comparison of height and the relationship between water levels at the AL-Rumaila gauging station and the VS.

2) Hydrological Estimation and Evaluation for Channel Creation on the Euphrates River

a) Hydrological Evaluation for Channel Creation at Coordinate (31.3351°N, 45.0527°E) on the Euphrates River

The hydrological feasibility of a channel constructed in the Euphrates River section at two coordinates of 31.3351°N, 45.0527°E and 31.314°N, 45.351°E is reviewed in this section. The channel size and discharge values were used to make estimates because there were not enough velocity measurements available in southern Iraq. In Hit, central Iraq, the historical discharge was recorded as 356 m^3/s. The estimated water velocity, given the river's width of 250 m and depth of 5 m, was approximately 0.285 m/s. In this case study, with a river section width of 64.7 m, depth of 5 m, and discharge rate of 550 m^3/s, a water velocity of 1.7 m/s was calculated at the beginning point between the Al-Hamza and Al-Rumaitha gauging stations (Figure 10). This indicates that the diversion channel (Figure 11) is viable at this site and corresponds to a cross-sectional area of 323.5 m^2.

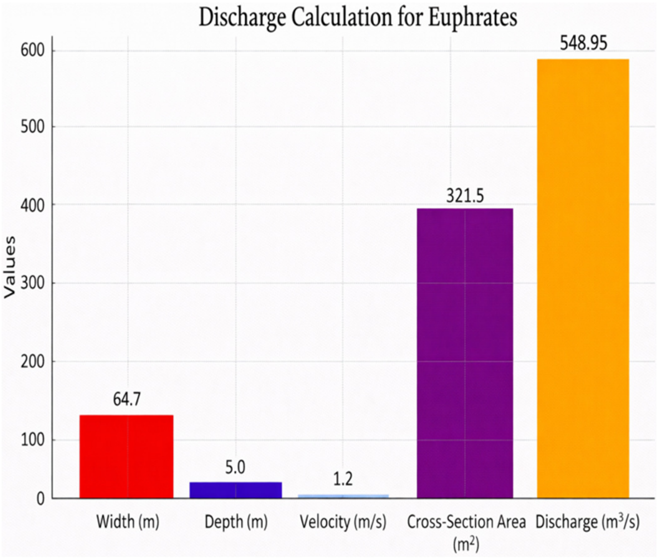

Fig. 10. Discharge was estimated based on depth and velocity at the Euphrates River at (31.3351, 45.0527).

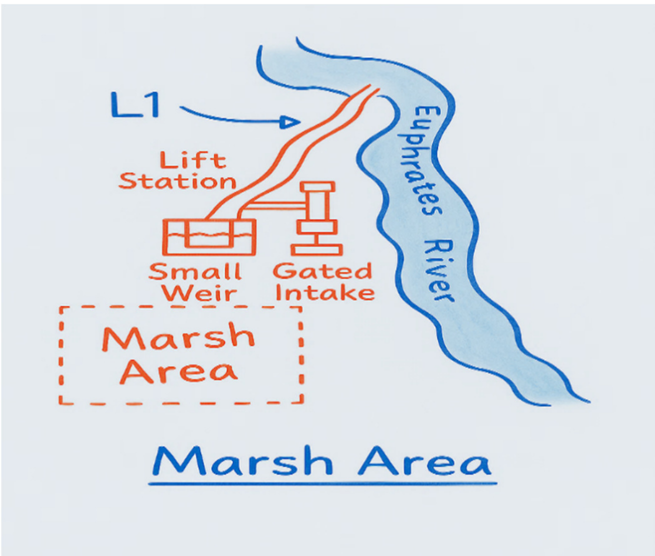

Fig. 11. Diagrammatic representation of the L1 distributary canal that branches off the Euphrates River with hydraulic control structures.

b) The Second Potential Section (31.314, 45.351) between Al-Rumaitha and Al-Khether Gauging Stations

The discharge was estimated at the second location (31.314, 45.351) using the Manning equation (9). The estimated volume of discharge, calculated at 165.83 m^3/s, was derived from the slope, width of 45 m, and mean depth of 5.205 m, which were determined using the difference in water level (Figure 12). Although this volume of water is insufficient to create a new river, it may provide some secondary channel sustenance through engineering. The findings support the creation of a diversion channel at point one, where appropriate devices, such as gated intakes or weirs, may be installed to regulate the flow, especially in the event of discharge fluctuation changes (Figure 11).

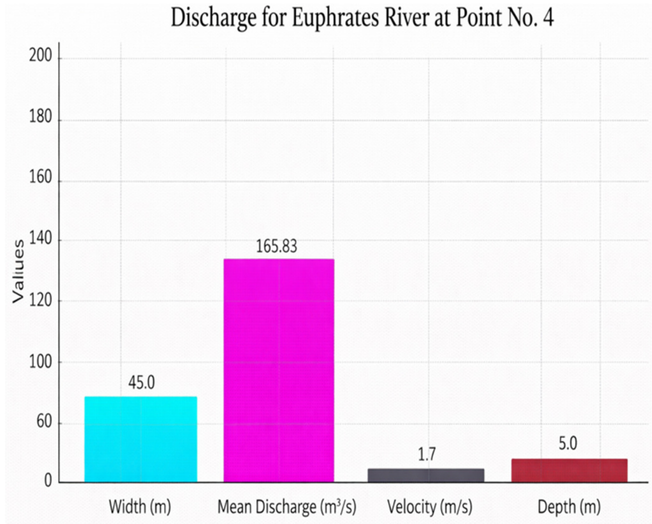

Fig. 12. The discharge between the Al-Rumaitha and Al-Khether gaugings.

c) Engineering, Hydrological, and Topographical Analysis of Proposed Canal Sites along the Euphrates River

The most promising location to start a new channel that would supply water to the arid and semi-arid regions of southwest Iraq is the area with coordinates of 31.3351°N 45.0527°E, according to the feasibility report on building a channel extension of the Euphrates River. The flow of 549.95 m^3/s at this point is regarded as moderate to high, indicating that there is sufficient water to divert. Furthermore, the river's 323.5 m^2 cross section is a sizable portion that may permit the construction of a diversion canal. Even if a flow rate of 1.7 m/s is acceptable, attention is needed to guarantee that the flow is continuous and flowing into the desert.

Figure 13 presents discharge estimates at two key locations along the Euphrates River in southern Iraq to aid in the hydrological feasibility analysis for potential canal construction. The discharge statistics for the point at coordinates 31.3351°N, 45.0527°E, with a river width of 64.7 m, depth of 5 m, and calculated velocity of 1.7 m/s. These figures yield a cross-sectional area of 323.5 m^2 and a discharge rate of around 549.95 m^3/s. This discharge is considered moderate to high, making it suitable for initiating a diversion channel in the adjacent marshlands or desert. The specific information supports the site's hydrological viability for canal construction due to its sufficient flow and regulated velocity. Conversely, point No. 4 is situated between the Al-Rumaitha and Al-Khether gauging stations at coordinates 31.314°N, 45.351°E on the Euphrates River. With a river width of 45 m and depth of 5 m, the discharge is much lower at 165.83 m^3/s, even if the flow velocity remains the same at 1.7 m/s. This suggests a restricted capacity for large-scale water redirection, even though a smaller controlled channel for irrigation or flood control may still be achievable with the correct technological techniques.

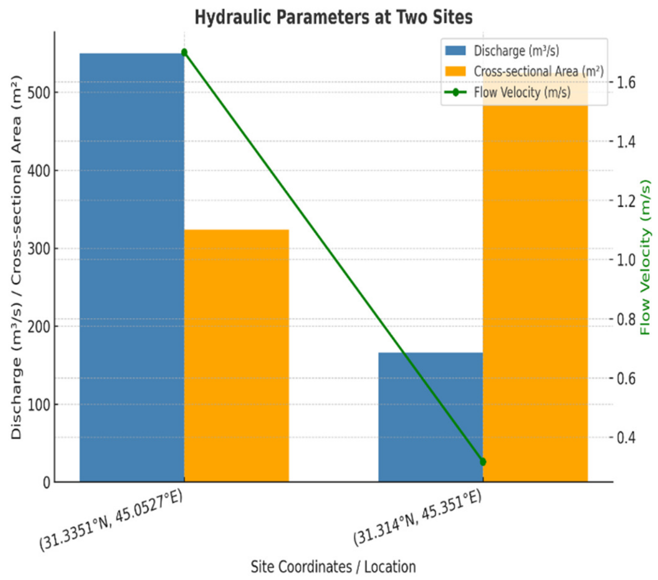

Fig. 13. Discharge levels at key potential locations along the Euphrates River for channel feasibility assessment.

Despite certain geographic difficulties, the location has a modest slope, which would help simplify the gravity-fed flow. To guarantee that a flow is maintained in places like level or sloping terrain, artificial pumping may be required. According to engineering practice, the channel must be built with gentle slopes to promote stability and reduce erosion. A small dam, weir, or gated intake is likely required at the site of division to regulate flow (Figure 14). Because frequent dredging is required, the silt deposition in the new branch must also be considered.

Fig. 14. The section illustrates the diversion system of the new channel located on the Euphrates River.

The correlation between discharge and cross-sectional area at specific Euphrates diversion locations is displayed in Figure 15. The proposed canal intake position is shown by the primary point that is highlighted (31.3351°N, 45.0527°E). The design of sustainable and effective channel dimensions for water diversion infrastructure is guided by the fact that larger discharges often demand larger cross-sectional areas.

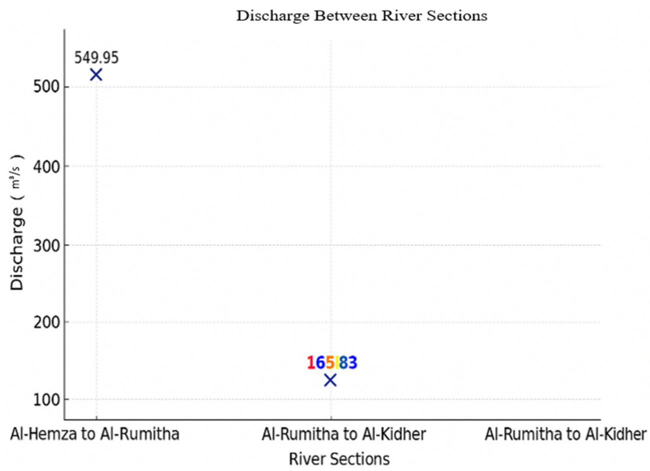

Fig. 15. Relationship between discharge and cross-sectional areas at key Euphrates locations for channel diversion feasibility.

B. Results for Applying the InSAR Technique

1) Evaluating and Analyzing DEM Data with RTKs

The performed comparison illustrates the effects of applying the stream-burning approach for increasing the accuracy and consistency of DEM 2024 with the field-recorded heights for the sixty locations in the study area. The elevation profiles of DEM 2024 almost matched the ground measurements with minimal deviations and an RMSE of 3.27 m, as portrayed in Figure 16. DEM 2024's remarkable reliability and homogeneity make it appropriate for a range of applications, including wetland mapping, which requires accurate terrain representation. Its low negative bias of -0.86 m and SD of 3.15, when compared to other DEMs in 2022 and 2023 (Table VI), indicate little understatement.

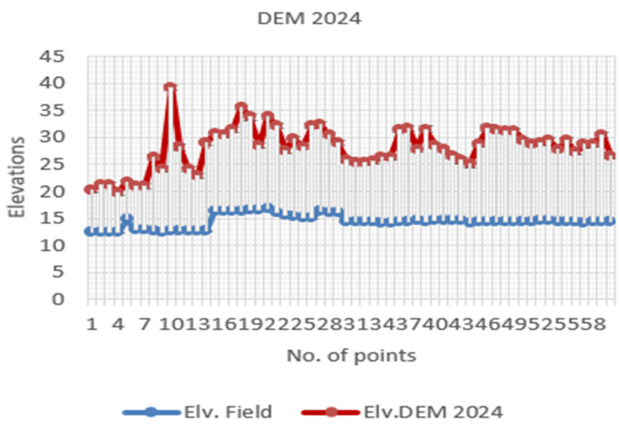

Fig. 16. Elevation profile comparison of DEM 2024 and RTK point measurements showing high correlation.

TABLE VI. STATISTICAL PARAMETERS FOR THE THREE DEMS FOR THE STUDY AREA

DEMs	DEM 2022	DEM 2023	DEM 2024
RMSE (m)	9.09	10.41	3.27
Bias (mean error) (m)	5.07	6.02	-0.86
SD (m)	7.54	8.49	3.15

This negative bias explains why DEM values are often somewhat lower than field-recorded altitudes. The histogram of errors indicates that most disparities are small and clustered near zero with no significant outliers (Figure 17). With the potential exception of a minor degree of calibration, the results generally support the use of the DEM as a trustworthy elevation reference for spatial analysis, planning, and modeling in the region under discussion. The distribution of elevation inaccuracies for the DEM-Field shows a negative bias of -0.86, centered slightly to the left of the zero.

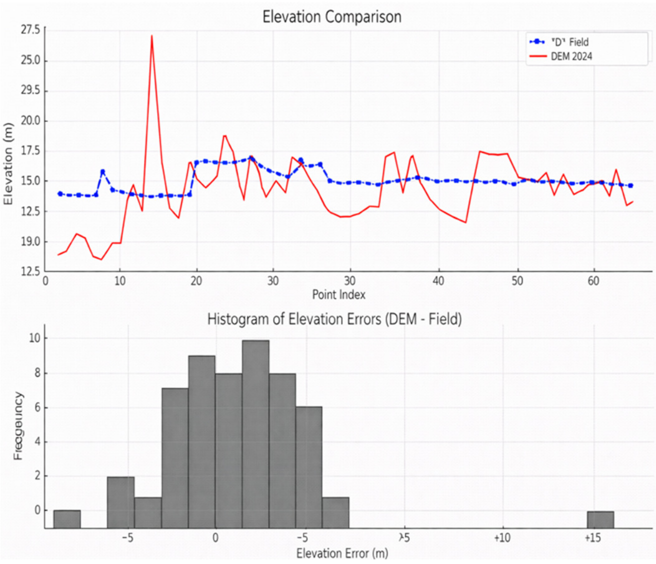

Fig. 17. Elevation profile comparison of DEM 2024 and RTK point measurements showing high correlation.

In the same context, two visual comparisons between the field-measured elevations and DEM 2024 data are shown in Figure 17. The elevation values for each surveyed site are displayed in the top graph. The red dashed line (Elv. DEM 2024) varies more than the blue solid line (Elv. Field), but it still closely follows the overall elevation trend. This shows a general agreement with a few small local variations. The distribution of elevation errors (DEM minus field values) is displayed in the bottom histogram. With a small skew and a few outliers, the majority of mistakes cluster around zero. This supports the conclusion that the DEM 2024 offers accurate elevation estimates with little variation from ground-truth data.

Moreover, the comparison error visualizations in Figure 18 demonstrate that among the three models, DEM 2024 has the least error distribution (Table VI). A smaller median error and wider interquartile range indicate higher-quality inputs or data processing. These results demonstrate that, compared to earlier DEM versions, DEM 2024 is a reliable elevation dataset with improved accuracy and consistency that may be utilized in spatial planning.

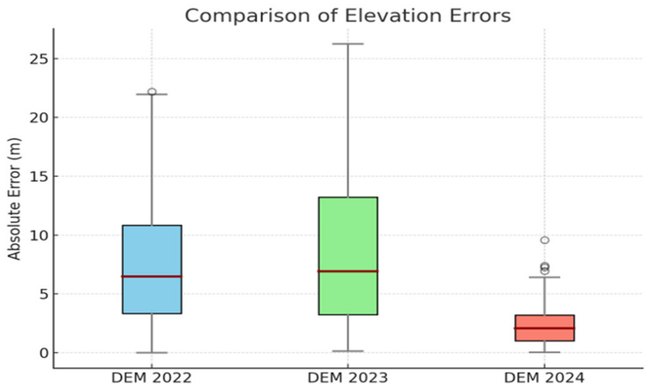

Fig. 18. Error visualizations illustrating the improvement in elevation accuracy across DEM versions 2022–2024, with the lowest error for DEM-2024.

2) Comparative Accuracy Assessment of DEMs (2022–2024) Using Statistical Error Metrics

According to the statistical analysis, DEM 2024 had the lowest bias (-0.86), lowest SD (3.15), and lowest RMSE (3.27), indicating excellent consistency and a small systematic error (Figure 19).

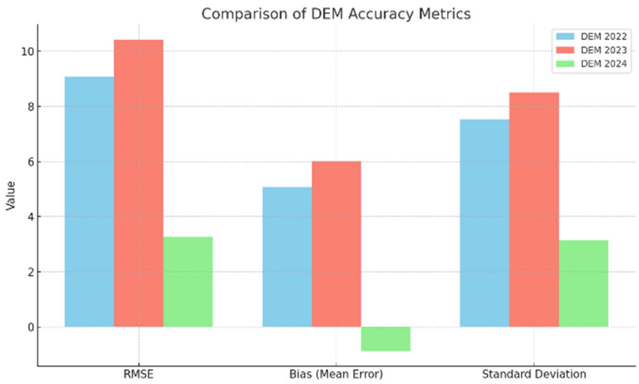

Fig. 19. A comparison of DEMs' accuracy from 2022 to 2024.

The low-lying, water-retentive areas and topographic interpretation will be more reliable because of DEM 2024's increased precision. In conclusion, DEM 2024 is the most advanced geographic research and environmental planning model, particularly suited for dry and semi-arid regions that require high accuracy. Both visual and numerical testing demonstrated that it is significantly superior in quality to earlier models.

3) Increasing Hydrological Accuracy for the DEM-2024 by Stream Burning Approach

In the arid and semi-arid regions of southern Iraq, the stream-burning approach significantly enhanced DEM 2024's ability to predict hydrological characteristics and locate possible marshland regions. The preliminary evaluation showed that DEM 2024 is the best elevation model, with elevation challenges ranging from 12.3 to 16.933 m, which are near-field measurements and ground-truth sites. Its accuracy was further supported by statistical criteria, such as a low RMSE (3.27 m), low bias (3.86 m), and low SD (3.15 m) when compared to the 2022 and 2023 DEMs.

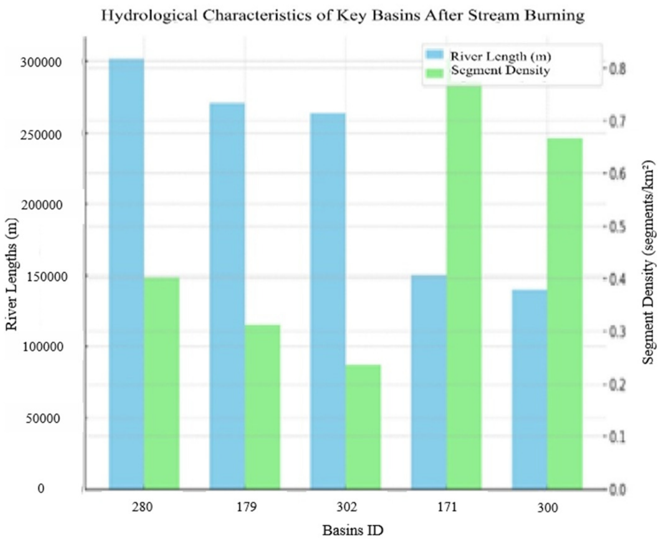

Fig. 20. Hydrological characteristics of key basins after applying the stream-burning technique.

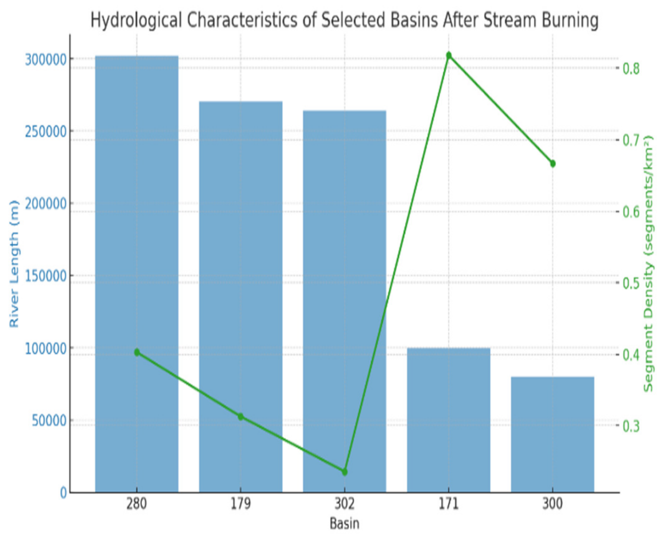

Fig. 21. River lengths and segment density comparison in five key basins after stream burning.

Stream burning, a preprocessing technique that includes sink filling, noise reduction, and hydrography information integration, made DEM 2024 a viable hydrological instrument. By connecting the modeled flow paths to actual river networks, the proposed approach improved water drainage and future prediction complexities while overcoming the limitations of DEM. Some important basins (280, 179, and 302) (Figure 20) were designated as large fields on which the marshland regions should be rebuilt because of the length of their rivers and the density of the stream segments. Basin 280, which has the longest river network (~301,647 m) and the highest density (0.403 segments/km^2) (Figure 21), was the fifth location with the highest potential for identification and restoration.

VII. DISCUSSION

A. *Quantitative Assessment of Marsh Identification and Creation Potential in Southwestern Iraq*

The probability of marsh creation can be predicted by examining the stream lengths in the hydrologic basins (segments) of the arid and semi-arid regions of southwestern Iraq. With a length of more than 160,000 m, the stream network in the extensive basins (280, 179, 302, and 300) exhibited a significant hydrological contribution and was suitable for marsh basin restoration. However, because of the poorly flowing surface water, basins 118, 134, and 148 with streams shorter than 8,000 m (Figure 22) also have limited prospects for opportunity. Seasonal wetlands may be constructed in mid-range basins (such as 159, 171, and 223). The findings of this study highlight the need for basin-specific initiatives that incorporate information on streams into ecological and land-use planning.

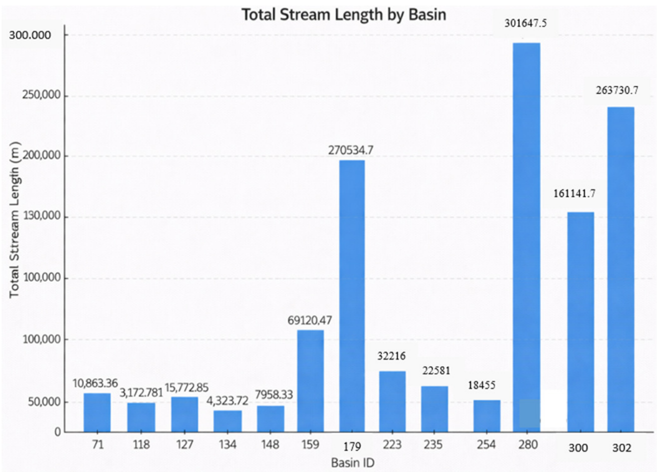

Fig. 22. The total lengths of the rivers inside the basins in the Southwest of Iraq.

1) *Spatial Distribution of River Origins in Arid and Semiarid Areas in Southwestern Iraq*

The distribution of river segments and stream lengths among the basins in southwest Iraq varies significantly, as shown in Figure 23 and Table VII. A basin has greater hydrological complexity and marsh growth potential when it contains more than 250 segments, particularly those with IDs 200 and 300. However, hydrological activity is low in basins with fewer than 50 segments. According to the quantitative data from the 2024 DEM, the area may be able to preserve wetlands during the dry season. Highly efficient drainage systems in other smaller basins, such as basins 280, 302, and 300, which have streams longer than 160,000 m, will help collect water and support the ecological rehabilitation of this delicate terrain.

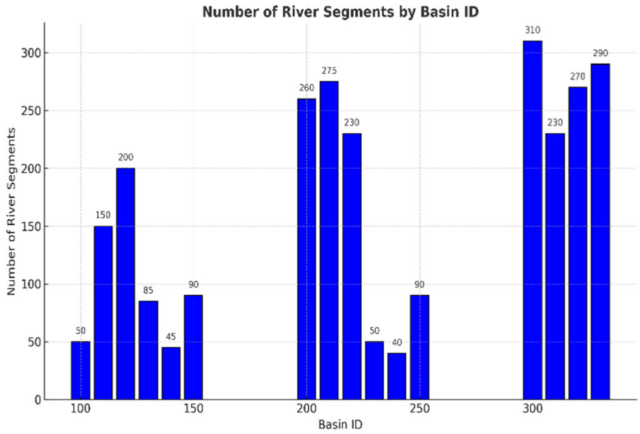

Fig. 23. Basin-wise distribution of river segments in the study area.

TABLE VII. TOTAL RIVER LENGTHS BY BASIN IN THE STUDY AREA OF THE ARID AND SEMIARID REGION IN SOUTHWESTERN IRAQ

Basin	Total length (m)
71	10863.36
118	3172.781
127	15772.85
134	4323.718
148	7958.332
159	34035.74
171	69120.47
179	270534.7
223	32216.58
235	22581.86
254	18455.64
263	20530.51
280	301647.5
288	10055.99
300	161141.7
302	263730.7

Despite Iraq's arid environment, the southwestern region contains several basins, including 179, 280, and 302 that exhibit significant stream patterns, demonstrating rich and widespread hydrological activity that sustains these basins. Smaller basins, such as 118 and 134, also encourage the development of isolated wetlands by directing surface water to form natural depressions. This study provides a visual map of these hydrological fluctuations.

In this study, the open-source software QGIS was used to create a river network in southwest Iraq. The enhanced DEM-2024 was utilized, which offers a topographic framework required for hydrological feature extraction and watershed delineation.

The river network was created using QGIS's spatial analysis tools, which employs elevation data to determine the total river length, flow accumulation, and drainage patterns, allowing for a quantitative evaluation of the drainage density and fluvial morphology. Additionally, the hydrological modeling plugin SAGA GIS in QGIS was utilized for extracting the river network (Figure 24). In the same context, QGIS combines several internal and external algorithms that can analyze stream networks and flow directions based on topographical features acquired from DEM-2024. To identify drainage channels, these procedures usually depend on D8 or D$^{\infty}$ flow direction algorithms, which are common methods in hydrological modeling and river network extraction.

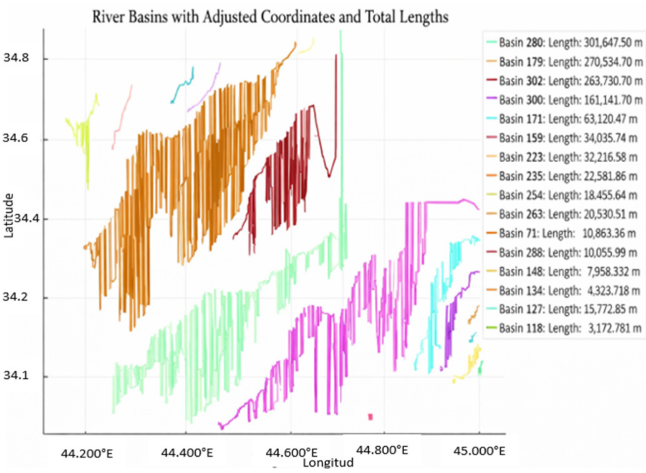

Fig. 24. The geographic distribution of the river.

The geographical distribution of river-starting places in Iraq's southern desert is presented in Figure 25. Most sites are roughly located between latitudes 34.18° N and 34.73° N and longitudes 44.345° E and 45.218° E. Marshes are created based on these coordinates, which are associated with important locations where the buildup of flow starts. The high concentration of river onsets, in locations around 44.6732° E longitude and 34.4° latitude, can be used to indicate the favorable runoff zones. The designated geographic layout supports long-term sustainability, restoration strategies, and regional water dynamics, and validates the viability of maintaining marsh ecosystems.

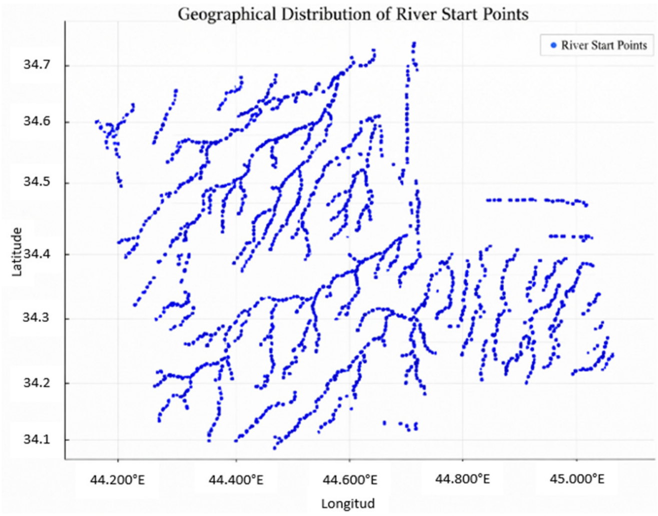

Fig. 25. The river starting locations on the enhanced DEM-2024.

2) Hydrological Connectivity and Stream Network Complexity in Key Basins Supporting Marsh Sustainability

Due to their well-established stream networks, basins 179, 280, and 302 in southern Iraq have great promise. With 328 fourth-order, 198 fifth-order, and 118 sixth-order streams, basin 280 is unique in that it has the greatest number of streams, indicating robust water storage and conveyance (Figure 26). To promote water circulation and increase the number of flood occurrences necessary to maintain a wetland, basins 179 and 302 are equally thick in hierarchy, with a large number of fourth- to sixth-order streams. However, basins like 71, 118, and 134 have extremely weak hydro-system architecture, making them unsuitable for marsh development.

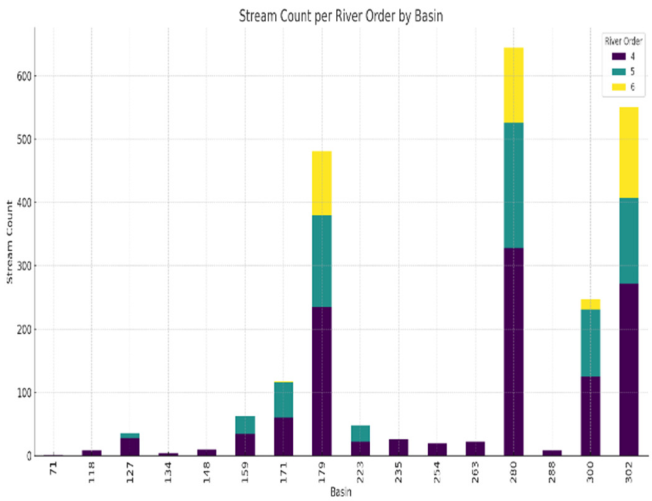

Fig. 26. The number of streams in each basin is displayed by river order.

Figure 27 presents the strength of the downstream link with a notable fifth-order and sixth-order flow and the dominance of fourth-order streams. When it comes to restoring and sustaining marshes in arid regions, this drainage complexity ensures efficient surface runoff collection and water retention.

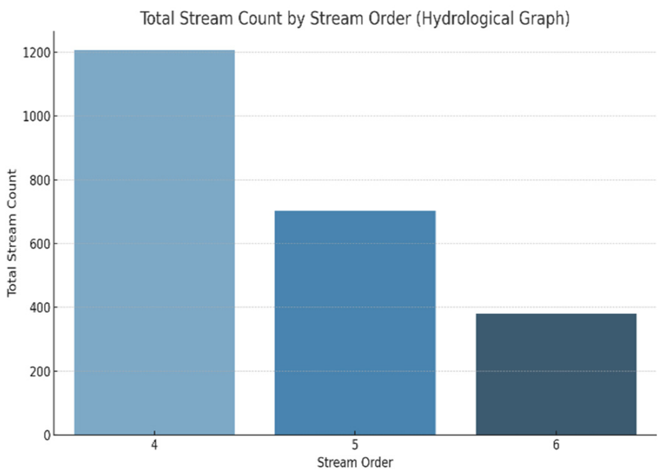

Fig. 27. Total stream counts in Southwestern Iraq by stream order.

3) DEM Reliability for Hydrological Analysis and Marsh Zone Identification Using Stream Burning

Basins 280 and 302 feature numerous river segments, indicating substantial hydrological circulation and potential water storage. Figure 28 illustrates the higher density and complexity of river segments per basin. With respect to wetland sustainability, the improved DEM makes it possible to more accurately identify basins that are hydrologically sustainable. For instance, basin 280 is the most suitable area for marsh growth because it has the longest river (~301,647 m) and the highest segment density (0.403 segments/km^2). Likewise, additional basins with appropriate flows and stream networks include basin 179 (~270,534 m, 0.313 density) and basin 302 (~263,730 m, 0.236 density). Because stream burning provides precise information about the lengths and quantities of streams, as well as basin hydrology, these results highlight the overall benefits of stream burning in terms of DMG data accuracy and its effectiveness in evaluating the potential for marsh restoration.

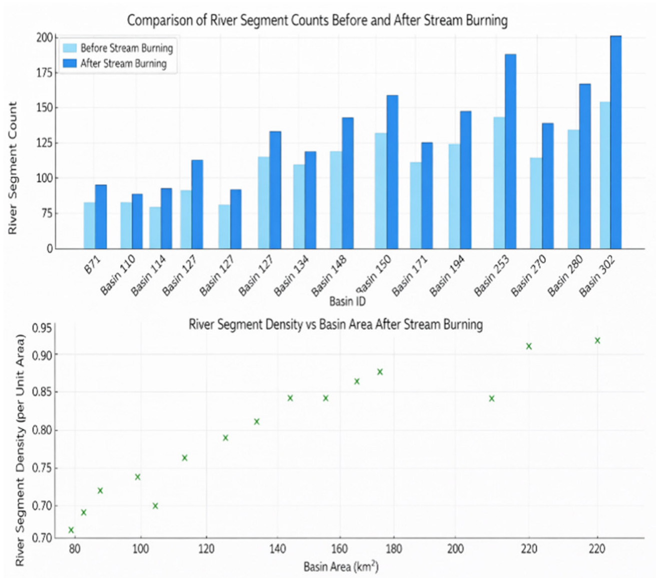

Fig. 28. Improved hydrological data by stream burning and increasing the density of river segments.

Stream-burning had a major positive effect on the hydrological accuracy of DEMs, unveiling patterns that are critical to the restoration of a marsh. The smaller basins, such as 171 and 300, are characterized by considerable segment density with short river length, which demonstrates possible limitations (Table VIII). In contrast, basin 280 is characterized by an expansive flow network and positive terrain. Improved flow accumulation modeling also facilitates accurate identification of the marsh home. Stream burning has greatly enhanced the overall DEM, as portrayed in Figure 29, with more flow accumulation in large basins, such as 280, 179, and 302, due to the intensity model. The basins affected by the Euphrates and the Tigris benefit from this method because it improves the spatial consistency and realism of the water flow by changing the heights along streams and using genuine hydrography data.

TABLE VIII. SEGMENT COUNT, AREA, AND DENSITY METRICS FOR SELECTED BASINS

Basin ID	Segments	Area (km^2)	Segment density (segments/km^2)
280	290	720	0.403
179	250	800	0.313
302	260	1100	0.236
300	180	270	0.667
171	90	110	0.818

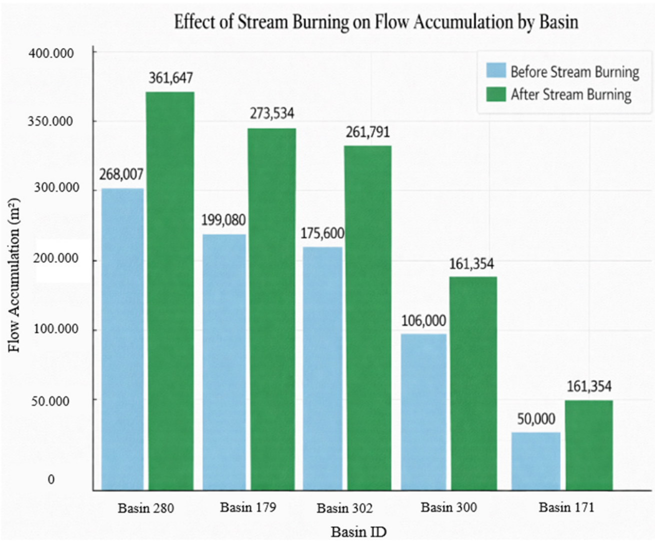

Fig. 29. Flow accumulation by basin before and after applying the stream-burning technique.

B. Spatial and Morphometric Characteristics of Major River Basins in the Marsh Area

Key morphometric measurements that show the hydrological behavior and marsh formation potential of the five major basins in the southern Iraqi desert are listed in Table IX. With a total area of 725.74 km^2 and the longest river network at 301.65 km, the semi-circular shape of basin 280 makes it ideal for retaining water and distributing flow evenly. It has a circularity ratio of 0.650 and a modest elongation ratio of 0.589. Basin 179, which covers 804.71 km^2, has a somewhat more elongated form (Re = 0.502) and a circularity ratio of 0.539, suggesting a moderate possibility of water accumulation and slower drainage. Basin 302, the largest at 1,116.83 km^2, has a large river network (263.73 km) with elongation and circularity ratios of 0.536 and 0.564, respectively, indicating steady hydrological activity and a high retention capacity. Basin 300 features a 161.14 km river network and excellent form characteristics (Re = 0.5485, Rc = 0.602), which boost its water storage capacity despite its smaller size of 254.23 km^2. Basin 171, the smallest at 121.37 km^2, also shows promising statistics with Re = 0.5176 and Rc = 0.511.

Together, these basins provide the ideal size, shape, and drainage characteristics for preserving marsh habitats. Their elongation and circularity ratios, which indicate relatively slow surface runoff and a greater likelihood of spontaneous pooling, make them great candidates for wetland restoration in dry and semi-arid conditions.

TABLE IX. SEGMENT COUNT, AREA, AND DENSITY METRICS FOR SELECTED BASINS

Basin ID	Area (km^2)	Perimeter (km)	Max length (km)	Elongation ratio	Circularity ratio	River length (km)
280	725.74	118.47	51.63	0.5888	0.6498	301.65
179	804.71	137.00	63.80	0.5017	0.5388	270.53
302	1116	157.77	70.30	0.5364	0.5639	263.73
300	254.23	72.85	32.80	0.5485	0.6020	161.14
171	121.37	54.64	24.02	0.5176	0.5109	69.12

Figure 30 compares the five major river basins in the research region in southwest Iraq based on key morphometric metrics, such as basin size, river length, elongation ratio, and circularity ratio. The largest areas and river lengths of basins 302 and 280 suggest large catchment systems with substantial surface water collection capabilities. Furthermore, these basins have modest circularity and elongation ratios, which are markers of basin shapes that encourage water retention and postpone runoff, two characteristics crucial to the development of marshes. However, basins such as 171 have less potential because of their smaller area and shorter river length.

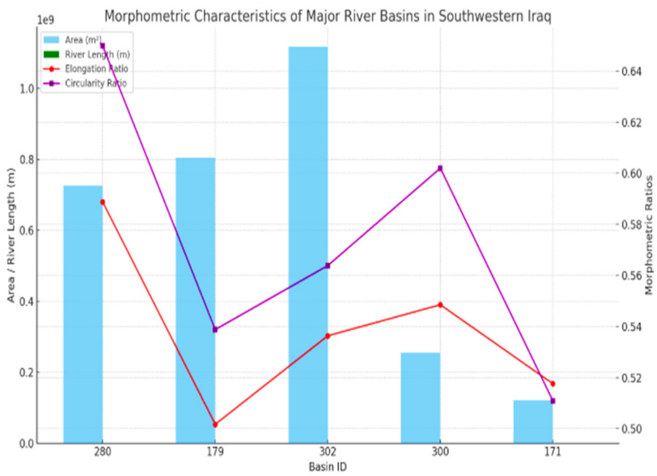

Fig. 30. The morphometric features of the main river basins in the southwest Iraq region.

The elongation and circularity ratios provide additional hydrological information. Specifically, larger circular basins tend to concentrate runoff more rapidly, whereas longer basins have more persistent flow. These morphometric characteristics help identify basins with hydrological patterns conducive to marsh formation. The strategic use of these basins may help with sustainable water resource management and the restoration of marsh ecosystems in arid regions.

VIII. CONCLUSIONS

Finding a suitable water supply and selecting a suitable marsh location are two essential engineering requirements for initiating long-term arid and semi-arid development in Iraq's southwestern desert. According to this study, the Euphrates River, which has a measured flow of 549.95 m^3/s at 31.3351°N and 45.0527°E, provides a long-term, steady, and exceptional water supply that supports the creation of marsh areas, agriculture, and ecosystem restoration in the study area. Because of this discharge rate, the marsh region identified in the study area may be consistently fed by a branching canal. The canal is 5.0 m deep, 64.7 m wide, and has a flow rate of 1.7 m/s.

Basin 280 is the ideal location for marsh development, according to hydrological and geomorphological research. Given that the total river length is 301,647.5 m and the total area of the basin is 725,742,984 m^2, there is a possibility that the wetlands in this basin might be significantly restored. The circularity ratio and the elongation ratios of basin 280 are 0.650 and 0.589, respectively, which show that it has a good capacity for water retention and distribution, with moderate compactness and form efficiency. The basin's extensive length (51,630.95 m) and perimeter (118,466.36 m) are additional elements that make its utilization beneficial since they provide a broad area that may be covered by flood control and ecological restoration.

The strategic location of basin 280, concerning the central route of the basin system and its proximity to the proposed intake station of the Euphrates River, lends credence to the hydraulic viability of channel construction in this area. Establishing a marsh in this area may support biodiversity, groundwater recharge, and climate resilience. Real-time data and satellite evaluations work together to ensure that the channel is aligned effectively, minimizing water loss and optimizing biological consequences. This suggests that to create sustainable wetlands, the flow capacity at 31.33510 °N and the physical characteristics of basin 280 must work in tandem.

Although the proposed channel shows promise for reducing desertification and recovering marsh regions in southwestern Iraq, further research is needed to determine its long-term feasibility. In order to fully assess system performance and guarantee sustainable water distribution throughout the designated wetland regions, future studies should incorporate geological stability, soil properties, and associated environmental elements.

ACKNOWLEDGMENTS

The authors would like to express their sincere gratitude to the Faculty of Built Environment and Surveying (FABU), Universiti Teknologi Malaysia (UTM), for their invaluable assistance, particularly in providing technical support and facilitating data collection for this study. The authors also gratefully acknowledge the financial support from Universiti Teknologi Malaysia through the UTM Contract MG Grant R.JI30000.7652.4C773 and the UTM Matching Grant Q.J130000.3052.04M83.

DECLARATION OF INTEREST STATEMENT

The authors declare that there are no conflicts of interest, whether financial, personal, or professional, which could be perceived to influence the work presented in this manuscript. All research was conducted with full academic integrity and objectivity, and no external interests have affected the analysis, interpretation, or presentation of the results.

REFERENCES

[1] S. Albhadili, I. A. Almallah, and S. T. Almulla, "Hydromorphometric Analysis of Wadi Al-Batin Alluvial Fan Using Remote Sensing and GIS Techniques, Southwestern Iraq," *The Iraqi Geological Journal*, vol. 55, no. 1F, pp. 134–150, June 2022, https://doi.org/10.46717/igj.55.1F.11Ms-2022-06-26.

[2] M. M. Chindo, M. Hashim, and A. W. Rasib, "Revising digital elevation models generation from Sentinel-1 synthetic aperture radar and interferometric technique in densely-vegetated humid tropical environment," *Geocarto International*, vol. 37, no. 27, pp. 18022–18041, Dec. 2022, https://doi.org/10.1080/10106049.2022.2136263.

[3] S. Dávila-Hernández *et al.*, "Effects of the Digital Elevation Model and Hydrological Processing Algorithms on the Geomorphological Parameterization," *Water*, vol. 14, no. 15, Jan. 2022, Art. no. 2363, https://doi.org/10.3390/w14152363.

[4] V. P. Yadav, R. Prasad, R. Bala, and A. K. Vishwakarma, "An improved inversion algorithm for spatio-temporal retrieval of soil moisture through modified water cloud model using C- band Sentinel-1A SAR data," *Computers and Electronics in Agriculture*, vol. 173, June 2020, Art. no. 105447, https://doi.org/10.1016/j.compag.2020.105447.

[5] A. Pepe and F. Calò, "A Review of Interferometric Synthetic Aperture RADAR (InSAR) Multi-Track Approaches for the Retrieval of Earth's Surface Displacements," *Applied Sciences*, vol. 7, no. 12, Dec. 2017, Art. no. 1264, https://doi.org/10.3390/app7121264.

[6] H. Li, J. Zhao, B. Yan, L. Yue, and L. Wang, "Global DEMs vary from one to another: an evaluation of newly released Copernicus, NASA and AW3D30 DEM on selected terrains of China using ICESat-2 altimetry data," *International Journal of Digital Earth*, vol. 15, no. 1, pp. 1149–1168, Dec. 2022, https://doi.org/10.1080/17538947.2022.2094002.

[7] Q. Du, L. I. Li, W. Peng, Y. Zhou, M. Chai, and J. Li, "Acquiring high-precision DEM in high altitude and cold area using InSAR technology," *Bulletin of Surveying and Mapping*, no. 3, 2021, Art. no. 44.

[8] Q. Chen, S. M. Mudd, M. Attal, and S. Hancock, "Extracting an accurate river network: Stream burning re-revisited," *Remote Sensing of Environment*, vol. 312, Oct. 2024, Art. no. 114333, https://doi.org/10.1016/j.rse.2024.114333.

[9] J. B. Lindsay, "The practice of DEM stream burning revisited," *Earth Surface Processes and Landforms*, vol. 41, no. 5, pp. 658–668, 2016, https://doi.org/10.1002/esp.3888.

[10] M. Halicki and T. Niedzielski, "The accuracy of the Sentinel-3A altimetry over Polish rivers," *Journal of Hydrology*, vol. 606, Mar. 2022, Art. no. 127355, https://doi.org/10.1016/j.jhydrol.2021.127355.

[11] S. Bogning *et al.*, "Monitoring Water Levels and Discharges Using Radar Altimetry in an Ungauged River Basin: The Case of the Ogooué," *Remote Sensing*, vol. 10, no. 2, Feb. 2018, Art. no. 350, https://doi.org/10.3390/rs10020350.

[12] C. Normandin *et al.*, "Evolution of the Performances of Radar Altimetry Missions from ERS-2 to Sentinel-3A over the Inner Niger Delta," *Remote Sensing*, vol. 10, no. 6, June 2018, Art. no. 833, https://doi.org/10.3390/rs10060833.

[13] S. Le Gac, F. Boy, D. Blumstein, L. Lasson, and N. Picot, "Benefits of the Open-Loop Tracking Command (OLTC): Extending conventional nadir altimetry to inland waters monitoring," *Advances in Space Research*, vol. 68, no. 2, pp. 843–852, July 2021, https://doi.org/10.1016/j.asr.2019.10.031.

[14] M. M. Hason, I. S. Abbood, and S. aldeen Odaa, "Land cover reflectance of Iraqi marshlands based on visible spectral multiband of satellite imagery," *Results in Engineering*, vol. 8, Dec. 2020, Art. no. 100167, https://doi.org/10.1016/j.rineng.2020.100167.

[15] M. Aryan and A. W. Bin Rasib, "Integration of interferometry and altimetry techniques for comping and reducing the desertification phenomena in Iraq," *IOP Conference Series: Earth and Environmental Science*, vol. 1274, Dec. 2023, Art. no. 012011, https://doi.org/10.1088/1755-1315/1274/1/012011.

[16] H. Shi, Y. Wu, Y. Shi, X. He, X. Zheng, and O. B. Andersen, "Enhanced Sea Surface Height Estimation With Interference Rejection Using High-Frequency Fully Focused SAR Altimetry Data Over Island Areas," *IEEE*

Transactions on Geoscience and Remote Sensing, vol. 63, 2025, Art. no. 4206216, https://doi.org/10.1109/TGRS.2025.3568079.

[17] F. S. Alrammahi, Q. H. M. Al-Madhlom, and S. A. Jassim, "Evaluation of Manning's Coefficients for the Al-Adhaim River Basin in Iraq utilizing Modern Techniques," *Engineering, Technology & Applied Science Research*, vol. 15, no. 2, pp. 21618–21626, Apr. 2025, https://doi.org/10.48084/etasr.10246.

[18] J. R. Al-Obaidi *et al.*, "The environmental, economic, and social development impact of desertification in Iraq: a review on desertification control measures and mitigation strategies," *Environmental Monitoring and Assessment*, vol. 194, no. 6, May 2022, Art. no. 440, https://doi.org/10.1007/s10661-022-10102-y.

[19] Z. Farooq Ahmed Fartm, "Desertification in Iraq and how to Combatit," *IOP Conference Series: Earth and Environmental Science*, vol. 553, Aug. 2020, Art. no. 012033, https://doi.org/10.1088/1755-1315/553/1/012033.

[20] S. Masia, A. Trabucco, D. Spano, R. L. Snyder, J. Sušnik, and S. Marras, "A modelling platform for climate change impact on local and regional crop water requirements," *Agricultural Water Management*, vol. 255, Sept. 2021, Art. no. 107005, https://doi.org/10.1016/j.agwat.2021.107005.